Stochastic gravitational-wave background from spin loss of black holes

Xi-Long Fan[1, *] and Yan-Bei Chen[2, †]

[1]*Department of Physics and Mechanical and Electrical Engineering, Hubei University of Education, Wuhan 430205, China*

[2]*Theoretical Astrophysics and the Burke Institute for Theoretical Physics, California Institute of Technology, Pasadena, CA 91125, USA*

Although spinning black holes are shown to be stable in vacuum in general relativity, there exists exotic mechanisms that can convert the spin energy of black holes into gravitational waves. Such waves may be very weak in amplitude, since the spin-down could take a long time, and a direct search may not be feasible. We propose to search for the stochastic background associated with the spin-down, and we relate the level of this background to the formation rate of spinning black holes from the merger of binary black holes, as well as the energy spectrum of waves emitted by the spin-down process. We argue that current LIGO-Virgo observations are not inconsistent with the existence of a spin-down process, as long as it is slow enough. On the other hand, the background may still exist as long as a moderate fraction of spin energy is emitted within Hubble time. This stochastic background could be one interesting target of next generation GW detector network, such as LIGO Voyager, and could be extracted from total stochastic background.

Introduction.– Spinning black holes are known to contain energy that can be extracted — even with classical physical processes (e.g. Penrose process [1] and Blandford-Znajek process [2]). The area theorem dictates a limit of extraction energy $\Delta E \leq M - M_{\rm irr}$, given by the difference between the mass M of the black hole, and its irreducible mass $M_{\rm irr}$ defined by:

$$M_{\rm irr} = \sqrt{\frac{1 + \sqrt{1-(a/M)^2}}{2}}M, \tag{1}$$

where a is the spin of the black hole [3]. This extraction is believed to be powering highly energetic astrophysical processes (e.g. [2]). More mathematically speaking, near spinning black holes, perturbations which enter the horizon that are co-rotating with the black hole, with a slower angular velocity, carries negative energy down the black hole, thereby transferring positive energy toward infinity.

This *superradiance* [4] effect causes perturbations to be *unstable* in some cases: (i) photons acquire mass due to dispersion when propagating through plasma [5, 6], (ii) for a massive scalar field [7], such as the axion and possibly other ultralight bosons [8–10], and (iii) if Kerr black hole transitions into an ultracompact object, or a *gravastar* [11, 12]. If a spinning black hole/gravastar were to form anyway, then this linear instability should lead to a Spin-Down (SD). In cases (ii) and (iii), this will lead to the conversion of spin energy into gravitational waves, through the re-radiation of gravitational waves by an axion or boson cloud in (ii), and through direct emission of gravitational waves in (iii).

The possibility of spin-down does not necessarily mean that isolated Kerr black holes, or spinning gravastars, do not exist in nature, since the instability rate can be low and the spin energy can take a long time to radiate away. In fact, significantly spinning black holes do form, e.g., due to binary black hole mergers, as so far have been detected by Advanced LIGO and Virgo [13–17], which estimates a local merger rate of 12-213 Gpc^{-3}yr^{-1} [15]. For equal-mass binaries, the final black hole has $a/M \approx 0.7$, with around 7% of its rest mass stored in spin energy, which is larger than the gravitational-wave energy radiated during the Inspiral, Merger and Ringdown (IMR) processes combined, which is roughly 5% [18]. In this way, if a non-trivial fraction of the spin energies of these newly formed black holes can be radiated away in the form of gravitational waves during Hubble time, such radiation will form a non-trivial, or even stronger, gravitational-wave background. We note that spin-down of Kerr black holes at a long time scale is consistent with current observations, since for the three pairs of merging black holes detected by Advanced LIGO and Advanced Virgo, the individual merging black holes may all have low or zero spins [15]. Since the IMR background is already plausible for detection in second-generation detector networks [19], and Advanced LIGO will be updated to Advanced LIGO + (AL+), LIGO Voyager (Voyager) [34], this additional background is well worth studying. We note that such a background from mechanism (ii) mentioned above has already been studied extensively in by Brito et al. [9, 10], but analysis here is intended for broader types of sources, and we directly attach our background to BBH mergers.

In this paper, we shall first set up models for the emission spectrum of a single BH merger remnant. We then compute the stochastic background using population models for binary coalescence throughout the age of the universe, and finally estimate whether the additional background can be detectable.

Emission from a single remnant.– For a binary of Schwarzschild black holes with masses $M_{1,2}$ and mass ratio $q \equiv M_1/M_2$, the spin a_0 and final mass M_0 of the new-born merged black hole has the following dependence on the symmetric mass ratio $\eta \equiv M_1M_2/(M_1+M_2)^2$ [20]:

$$\frac{a_0}{M_0} = 2\sqrt{3}\eta - 3.454\eta^2 + 2.353\eta^3. \tag{2}$$

Assuming that all spin energy is radiated as gravitational waves, we obtain the spin-down energy :

$$\Delta E^{\rm SD}_{\rm tot} = M - M_{\rm irr} = \left(1 - \sqrt{\frac{1+\sqrt{1-\alpha^2}}{2}}\right)M, \tag{3}$$

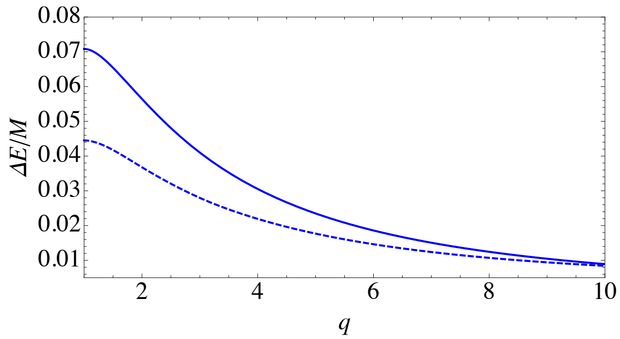

FIG. 1: Energy stored in the spin of the final merger product (solid line), in comparison with energy radiated during the entire coalescence (dashed line).

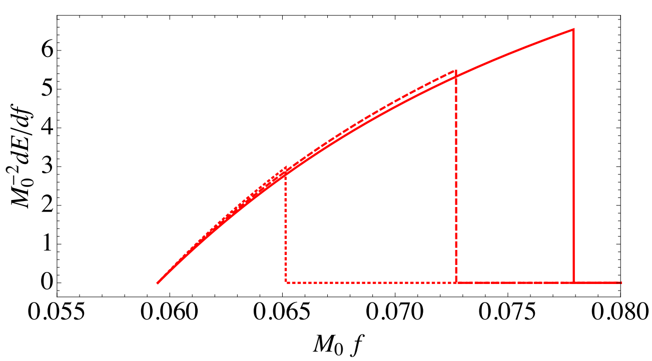

FIG. 2: Radiation spectrum during the spin decay process, assuming that radiation is predominantly at the first QNM of the merger product, for mass ratio $q = 1$ (solid), 3 (dashed) and 10 (dotted).

where $\alpha \equiv a/M$ is the dimensionless spin. As indicated by Fig. 1, for comparable masses (with mass ratio q close to unity), $\Delta E_{\rm tot}^{\rm SD}$ is always significantly larger than $\Delta E_{\rm tot}^{\rm IMR}$ [21].

In the following, we shall make two different models for the frequency spectrum $dE^{\rm SD}/df$. The simplest model would be a Gaussian,

$$\left(\frac{dE^{\rm SD}}{df}\right)_{\rm Gauss} = \frac{\Delta E_{\rm tot}^{\rm SD}}{\sqrt{2\pi} f_c/q} \exp\left[-\frac{(f-f_c)^2}{2(f_c/Q)^2}\right], \tag{4}$$

where f_c is the central frequency, which we will prescribe to be $f_c = \beta/M$, with β a (mass- and spin-independent) constant, and Q is a constant quality factor. We shall refer to this as the Gaussian model.

As another model, let us assume that at any given moment, the emission is only at the lowest quasi-normal mode (QNM) frequency of the Kerr black hole,

$$f_{\rm QNM}(M,a) = M^{-1} F(a/M), \tag{5}$$

where F is given by, e.g., Eq. (4.4) of Ref. [22]. We shall refer to this as the QNM model, and it will be part of our *fiducial model*. Assuming that $M_{\rm irr}$ remains the same throughout the spin-down process, we obtain

$$\left(\frac{dE^{\rm SD}}{df}\right)_{\rm QNM} = \left[\frac{\partial M}{\partial \alpha}\right]_{M_{\rm irr}} \Big/ \left[\frac{\partial f_{\rm QNM}}{\partial \alpha}\right]_{M_{\rm irr}}, \tag{6}$$

where both M and $f_{\rm QNM}$ are written in terms of $M_{\rm irr}$ and α :

$$M(M_{\rm irr},\alpha) = M_{\rm irr}/\sqrt{1+\sqrt{1-\alpha^2}}, \tag{7}$$

and

$$f_{\rm QNM}(M_{\rm irr},\alpha) = \sqrt{1+\sqrt{1-\alpha^2}} M_{\rm irr}^{-1} F(\alpha). \tag{8}$$

For a new-born merged black hole with mass M_0 and dimensionless spin α_0, we first compute $M_{\rm irr}$, which remains fixed during the spin-down, then obtain both f and dE/df as functions of α, with α decreasing from α_0 to 0. In Fig. 2, we plot $M_0^{-2}(dE^{\rm SD}/df)_{\rm QNM}$ as functions of $M_0 f$, for Kerr black holes that form from binaries with q =1, 3 and 10, with α =0.69, 0.54 and 0.26, respectively.

Stochastic Background.– By using knowledge about cosmology and binary black-hole merger rate throughout ages of the universe, the energy spectrum of the spin-down of the final black hole produced by a single binary merger can be converted into the energy density spectrum of the stochastic background, which we express in terms of the energy density per logarithmic frequency band, normalized by the closing energy density of the universe [19, 23]:

$$\Omega_{\rm GW}(f_{\rm obs}) \equiv \rho_c{}^{-1}\left[d\rho(f)/d\log f\right]_{f=f_{\rm obs}}$$
$$= \int d\theta \int_0^{z_{\rm max}} dz \frac{f_{\rm obs} R_m(z,\theta)\left[\frac{dE(f,\theta)}{df}\right]_{f=(1+z)f_{\rm obs}}}{(1+z)\rho_c H_0 E(\Omega_M,\Omega_\Lambda,z)}. \tag{9}$$

Here we assume a family of sources parametrized by θ (e.g., masses and spins), with $R_m(z,\theta)$ the event rate density per θ volume, per co-moving volume at redshift z, and $E(\Omega_M,\Omega_\Lambda,z) = \sqrt{\Omega_M(1+z)^3+\Omega_\Lambda}$ [24]. We use $H_0 = 70$ km s^{-1} Mpc^{-1}, $\Omega_M = 1-\Omega_\Lambda = 0.28$ in this paper [25]. For each z, one can define

$$\mathcal{R}_m(z) = \int R_m(z,\theta)\, d\theta, \quad p(z,\theta) = R(z,\theta)/\mathcal{R}_m(z) \tag{10}$$

with $\mathcal{R}_m(z)$ the total rate per unit co-moving volume at redshift z, and $p(z,\theta)$ the distribution density of source parameter θ at redshift z.

Detectability.– The optimal signal-to-noise ratio (SNR) for the the total background energy density spectrum is given by

$$\mathrm{SNR} = \frac{3H_0^2}{10\pi^2}\sqrt{2T}\left[\int_0^\infty df \sum_{i>j}\frac{\gamma_{ij}^2(f)\Omega_{\rm GW}^2(f)}{f^6 S_h^i(f) S_h^j(f)}\right]^{1/2}, \tag{11}$$

for a network of detectors $i,j = 1,2,\cdots,n$, where $S_h^i(f)$ is the one-sided strain noise spectral density of detector i; $\gamma_{ij}(f)$ is the *normalized isotropic overlap reduction function* between the i and j detectors, and T is the accumulated coincident observation time of detectors. To detect a stochastic background with 90% and 99.7% confidence, the SNR should be larger than 1.65 and 3, respectively [23]. Note that this SNR is only

Network	IMR	SD	IMR+SD
AL+	7.7436	1.0579	7.9587
AL+ (100-200)	0.3637	0.6103	0.9740
Voyager	54.7418	4.4315	55.2951
Voyager (100-200)	1.4722	2.4326	3.9047

TABLE I: The network SNR for *fiducial* IMR alone, spin-down alone, and both combined, for networks combining AL+, Voyager. The first and third lines show the optimal SNR. The second and forth lines show the SNR with 100-200 Hz band-pass filter.

achievable when our template for the shape of $\Omega_{\rm GW}(f)$ is optimal.

As we see from Eq. (9), the total energy density spectrum $\Omega_{\rm GW}$ mainly depends on the merger rate of one class of source $\mathcal{R}_m$, source population properties (such as mass distribution) $p(z,\theta)$ and the spectral energy density of a single source dE/df. The detail effects of merger rate and source mass distribution are discussed in [19, 26]. These two ingredients have weak effects on the background spectrum shape, especially in the Advanced LIGO- Advanced Virgo network band 10-50 Hz, where the spectrum is well approximated by a power law $\Omega_{\rm GW} \sim f^{2/3}$ (see detail discussion and references in [19, 27]). Note that, the spectral energy density $(dE/df)_{\rm IMR}$ of single source adopted in most literature is only the leading harmonic of the GW signal (e.g.[19, 28]), which is reasonable for current ground detectors, since the overlap reduction function modified the most sensitive band to 10-50 Hz. Our *fiducial* QNM model is constructed as follows: (i) we assume $\mathcal{R}_m(z)$ to be proportional to the cosmic star formation rates ([29]) with a constant time delay (3.65 Gyr) between the star formation and binary black hole merger [30] and normalized to $\mathcal{R}_m(0) = 28\,{\rm Gpc}^{-3}\,{\rm yr}^{-1}$ (see detail in [31]). (ii) we adopt a uniform distribution for $10M_\odot < M_{1,2} < 30M_\odot$ for $\theta = (M_1, M_2)$, (iii) we adopt $(dE/df)_{\rm IMR}$ [28] for the IMR parts of the waveform superimpose $(dE^{\rm SD}/df)_{\rm QNM}$ directly as an additional contribution.

The detection ability of a background of a detector network also depends on the overlap reduction function. In Fig. 3, we plot contributions to $\Omega_{\rm GW}$ from inspiral, merger, ringdown, as well as from spin-down, in comparison with

$$\Omega_* \equiv \frac{S_h^{\rm AdvLIGO} f^3}{\gamma_{\rm HL}} \sqrt{\frac{1}{2\Delta f T}}\, \frac{10\pi^2}{3H_0^2}\,, \qquad (12)$$

which sets 1-σ sensitivity to Ω_{GW} in each frequency bin [32]. Here $\gamma_{\rm HL}$ is the overlap reduction function between the Hanford and Livingston sites of LIGO.

In Table I, we show the 1-year *optimal* SNR for Advanced LIGO+ (first row) and LIGO Voyager (third row), assuming a stochastic background from IMR, SD and IMR+SD, and an optimal filter that corresponds to each case; the *fiducial* QNM model is used. Even though the SD component does contain more energy than the IMR component, and the emissions are within the detection band of ground-based detectors, the existence of an addition SD only leads to a small increase in SNR

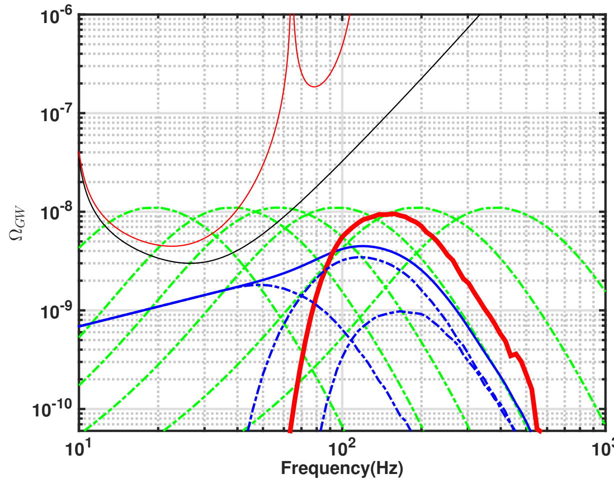

FIG. 3: We present a set of potential spectra for a BBH background using the flat mass distribution model with the local rate inferred from the O1 and O2 detections. The thick red line represents the *fiducial* QNM model of the spindown mechanism. The blue dashed line represents the inspiral, merger and ringdown mechanism and blue line present the total IMR background. The alternative models of the spin-down mechanism are shown in green dashed lines assuming different predominant central frequency (from let to right are the Gaussian model with $Q = 3$ and β= $0.01, 0.02, 0.03, 0.05, 0.1, 0.2$). The thin red and black curve shows the one year sensitivity Ω_* of designed Advanced LIGO network and two co-located and co-aligned Advanced LIGO like detectors, respectively (see Eq. (12)).

of around 3% — because $\gamma_{\rm HL}$ significantly decreases above ~50 Hz.

Extracting the SD background.– To see that the additional SD background is in fact detectable, we apply a bandpass filter between 100 Hz and 200 Hz, and the corresponding SNRs are listed on the second and fourth rows of Table I. In this band, the gap is more significant. For LIGO Voyager, the IMR+SD background has a SNR greater than 3, which makes it detectable with greater than 99.7% confidence, while the SNR for IMR alone is under the 90% detectability threshold.

More quantitatively, we can use a Fisher Matrix formalism to obtain the parameter estimation error for the amplitude of the SD background. Suppose the output of each detector is given by $x_i(f) = n_i(f) + h_i(f)$ where n_i is the noise and h_i the gravitational-wave signal, we construct the correlation between each pair of detectors: $z_{ij}(f) = x_i^*(f)x_j(f)$. The expectation value of z_{ij} is given by

$$\langle z_{ij}(f)\rangle = \langle h_i^*(f)h_j(f)\rangle = \frac{3H_0^2 T\gamma_{ij}(f)}{20\pi^2 f^3}\Omega^{\rm GW}(f) \equiv c_{ij}(f) \quad (13)$$

The covariance matrix is given by

$$\begin{aligned} &\langle z_{ij}^*(f')z_{lm}(f)\rangle - \langle z_{ij}^*(f')\rangle\langle z_{lm}(f)\rangle \\ \approx\ &\langle n_i(f')n_j^*(f')n_l^*(f)n_m(f)\rangle \\ =\ &\frac{1}{4}(\delta_{il}\delta_{jm} + \delta_{im}\delta_{jl})TS_l(f)S_m(f)\delta(f-f') \qquad (14) \end{aligned}$$

In fact, we only need to consider z_{ij} with $i > j$, which means the $z_{ij}(f)$'s all have independent noise, and the likelihood function for a particular $z_{ij}(f)$ is given by [33]

$$p[z_{ij}(f)|S_h(f)] \propto \exp\left[-\int_0^{+\infty} \frac{4|z_{ij}(f) - c_{ij}(f)|^2}{TS_i(f)S_j(f)} df\right] \quad (15)$$

If we only consider the SNR, we will simply sum all the frequencies and detector pairs by quadrature, and take the square root, and obtain

$$\mathrm{SNR} = \left[\sum_{i>j} 8 \int_0^{+\infty} df \frac{c_{ij}^2}{TS_i(f)S_j(f)}\right]^{1/2} \quad (16)$$

which agrees with Eq. (11). Suppose Ω_{GW} depends on a set of parameters θ^α, then we can obtain the Fisher matrix

$$\Gamma_{\alpha\beta} = \left(\frac{3H_0^2\sqrt{2T}}{10\pi^2}\right)^2 \sum_{i>j} \int_0^{+\infty} df \frac{\gamma_{ij}^2}{f^6 S_i^h S_j^h} \frac{\partial \Omega^{\mathrm{GW}}}{\partial \theta^\alpha} \frac{\partial \Omega^{\mathrm{GW}}}{\partial \theta^\beta} . \quad (17)$$

Suppose we have a simple model with

$$\Omega^{\mathrm{GW}} = \sum_J \alpha_J \Omega_J \quad (18)$$

where in our case J is for IMR and SD. We obtain

$$\Gamma_{JK} = \left(\frac{3H_0^2\sqrt{2T}}{10\pi^2}\right)^2 \sum_{i>j} \int_0^{+\infty} df \frac{\gamma_{ij}^2 \Omega_J \Omega_K}{f^6 S_i^h S_j^h} \quad (19)$$

and the estimation error is given by

$$\Delta\alpha_{\mathrm{SD}} = \left(\Gamma_{\mathrm{SD,SD}} - \Gamma_{\mathrm{SD,IMR}}^2 / \Gamma_{\mathrm{IMR,IMR}}\right)^{-1} \quad (20)$$

In Fig. 4, we plot $\Delta\alpha_{\mathrm{SD}}$ for Gaussian models with different values of β and Q, and *fiducial* models. The estimation of the amplitude SD models depends on the predominant central frequency. When the SD model and IRM model have spectra that are well separated in the frequency domain, the $\Gamma_{\mathrm{SD,IMR}} \sim 0$, then $\mathrm{SNR}_{SD} \sim \sqrt{\Delta\alpha_{\mathrm{SD}}^{-1}}$. The dominant central frequency of the *fiducial model* is quite different from the IRM model (see Fig. 3), therefore $\Delta\alpha_{\mathrm{SD}} = 0.0513$ is consistent with the SNR (Eq. (11)) shown in Table. I. In the most sensitive band, the spectra shape of Gaussian models (e.g. $\beta < 0.1$) is quite distinguishable from the power law shape of the IMR model. In this case, the estimation error of the amplitude of the SD background is < 10%.

Conclusion and outlook.– In this paper, we argued that spinning black holes, or ultracompact objects, can spin down without being inconsistent with LIGO observations — as long as the spin-down rate is much longer than the dynamical time scales of the black holes. Because spinning black holes (or ultracompact objects) do form, as indicated by LIGO observations, and because spinning black holes carry significant amount of spin energy such spin down can give rise to a detectable stochastic gravitational-wave background. Since the mechanisms of such spin-downs can be quite speculative,

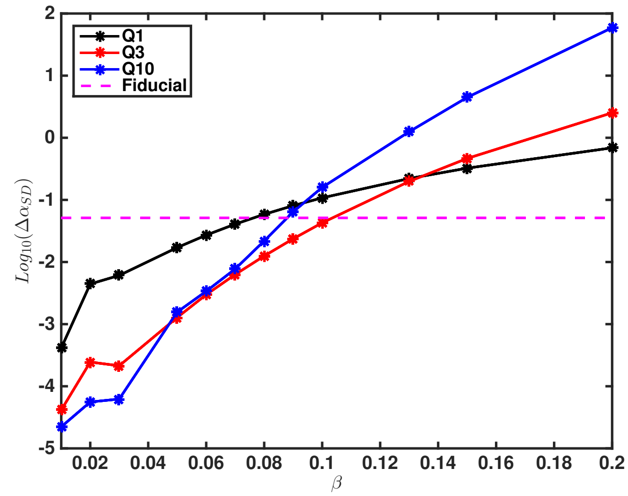

FIG. 4: The estimation error $\Delta\alpha_{\mathrm{SD}}$ for one year Voyager observation for SD models. Q1, Q3 and Q10 represent Gaussian model with quality factor Q=1, 3 and 10, respectively.

with details of the waveforms uncertain, searching for such a stochastic background seems the most appropriate way to look for their existence. The search's strategy could be to measure the contributions of models to measured SNR with band-pass filters. This BH spin-down stochastic background could be one interesting target of next generation GW detector network, such as Voyager. The parameter estimation error for the amplitude of the detectable SD backgrounds is < 10% for 1-year observation of Voyager estimated by our proposed Fisher Matrix formalism approach.

Acknowledgments.— We thanks A. Matas for valuable comments. X. F. is supported by Natural Science Foundation of China under Grants (No. 11633001, No. 11673008) and Newton International Fellowship Alumni Follow on Funding. Y. C. is supported by US NSF Grant PHY-1708212 and PHY-1404569 and PHY-1708213.

* Electronic address: fanxilong@outlook.com
† Electronic address: yanbei@caltech.edu

[1] R. Penrose and R. M. Floyd, Nature Physical Science **229**, 177 (1971).
[2] R. D. Blandford and R. L. Znajek, Monthly Notices of the Royal Astronomical Society **179**, 433 (1977).
[3] D. Christodoulou, Phys. Rev. Lett. **25**, 1596 (1970), URL `https://link.aps.org/doi/10.1103/PhysRevLett.25.1596`.
[4] W. H. Press and S. A. Teukolsky, Nature **238**, 211 (1972).
[5] S. A. Teukolsky and W. Press, The Astrophysical Journal **193**, 443 (1974).
[6] J. P. Conlon and C. A. Herdeiro, arXiv preprint arXiv:1701.02034 (2017).
[7] S. Detweiler, Physical Review D **22**, 2323 (1980).
[8] A. Arvanitaki and S. Dubovsky, Phys. Rev. D **83**, 044026 (2011), URL `https://link.aps.org/doi/10.1103/`

PhysRevD.83.044026.

[9] R. Brito, S. Ghosh, E. Barausse, E. Berti, V. Cardoso, I. Dvorkin, A. Klein, and P. Pani, Physical Review Letters **119**, 131101 (2017), 1706.05097.

[10] R. Brito, S. Ghosh, E. Barausse, E. Berti, V. Cardoso, I. Dvorkin, A. Klein, and P. Pani, Phys. Rev. D **96**, 064050 (2017), URL https://link.aps.org/doi/10.1103/PhysRevD.96.064050.

[11] C. B. Chirenti and L. Rezzolla, Physical Review D **78**, 084011 (2008).

[12] V. Cardoso, P. Pani, M. Cadoni, and M. Cavaglia, Physical Review D **77**, 124044 (2008).

[13] B. P. Abbott, R. Abbott, T. D. Abbott, M. R. Abernathy, F. Acernese, K. Ackley, C. Adams, T. Adams, P. Addesso, R. X. Adhikari, et al., Physical Review Letters **116**, 061102 (2016), 1602.03837.

[14] B. P. Abbott, R. Abbott, T. D. Abbott, M. R. Abernathy, F. Acernese, K. Ackley, C. Adams, T. Adams, P. Addesso, R. X. Adhikari, et al., Physical Review Letters **116**, 241103 (2016), 1606.04855.

[15] The LIGO Scientific Collaboration, the Virgo Collaboration, B. P. Abbott, R. Abbott, T. D. Abbott, F. Acernese, K. Ackley, C. Adams, T. Adams, P. Addesso, et al., Physical Review Letters **118**, 221101 (2017), 1706.01812.

[16] The LIGO Scientific Collaboration, the Virgo Collaboration, B. P. Abbott, R. Abbott, T. D. Abbott, F. Acernese, K. Ackley, C. Adams, T. Adams, P. Addesso, et al., ArXiv e-prints (2017), 1711.05578.

[17] B. P. Abbott, R. Abbott, T. D. Abbott, F. Acernese, K. Ackley, C. Adams, T. Adams, P. Addesso, R. X. Adhikari, V. B. Adya, et al., Physical Review Letters **119**, 141101 (2017), 1709.09660.

[18] F. Pretorius, Phys. Rev. Lett. **95**, 121101 (2005), URL https://link.aps.org/doi/10.1103/PhysRevLett.95.121101.

[19] B. P. Abbott, R. Abbott, T. D. Abbott, M. R. Abernathy, F. Acernese, K. Ackley, C. Adams, T. Adams, P. Addesso, R. X. Adhikari, et al., Physical Review Letters **116**, 131102 (2016), 1602.03847.

[20] L. Rezzolla, P. Diener, E. N. Dorband, D. Pollney, C. Reisswig, E. Schnetter, and J. Seiler, The Astrophysical Journal Letters **674**, L29 (2008).

[21] J. Healy, C. O. Lousto, and Y. Zlochower, Phys. Rev. D **90**, 104004 (2014), URL https://link.aps.org/doi/10.1103/PhysRevD.90.104004.

[22] F. Echeverria, Phys. Rev. D **40**, 3194 (1989).

[23] B. Allen and J. D. Romano, Phys. Rev. D **59**, 102001 (1999), gr-qc/9710117.

[24] D. W. Hogg, ArXiv Astrophysics e-prints (1999), astro-ph/9905116.

[25] C. L. Bennett, D. Larson, J. L. Weiland, N. Jarosik, G. Hinshaw, N. Odegard, K. M. Smith, R. S. Hill, B. Gold, M. Halpern, et al., The Astrophysical Journal Supplement **208**, 20 (2013), 1212.5225.

[26] B. P. Abbott, R. Abbott, T. D. Abbott, M. R. Abernathy, F. Acernese, K. Ackley, C. Adams, T. Adams, P. Addesso, R. X. Adhikari, et al., Physical Review Letters **118**, 121101 (2017), 1612.02029.

[27] X.-J. Zhu, E. J. Howell, D. G. Blair, and Z.-H. Zhu, Monthly Notices of the Royal Astronomical Society **431**, 882 (2013), 1209.0595.

[28] P. Ajith, Phys. Rev. D **84**, 084037 (2011), 1107.1267.

[29] B. E. Robertson and R. S. Ellis, Astrophys. J. **744**, 95 (2012), 1109.0990.

[30] D. Wanderman and T. Piran, Monthly Notices of the Royal Astronomical Society **448**, 3026 (2015), 1405.5878.

[31] W. Tan, X. Fan, and F. Wang, in prepare (2017).

[32] J. D. Romano and N. J. Cornish, Living Reviews in Relativity **20**, 2 (2017), 1608.06889.

[33] J. D. Romano and N. J. Cornish, Living Reviews in Relativity **20**, 2 (2017), ISSN 1433-8351, URL https://doi.org/10.1007/s41114-017-0004-1.

[34] LIGO Document T1500293-v8 and LIGO Document T1700231-v3